COMMUNICATION

A new structured aluminium–air secondary battery with a ceramic aluminium ion conductor

Ryohei Mori*

A metal–air secondary cell with the abundant metal aluminium has been assembled by placing the aluminium ion conductor $Al_2(WO_4)_3$ both on top of the aluminium anode and underneath the air cathode. This provides a snapshot of future Al–air batteries.

New solutions and materials for high energy and power density storage are required to meet the increasing demand for competitive (hybrid) electric vehicles, (H)EVs; existing nickel metal hydride and lithium-ion cell technologies fall short in terms of price, range, charge time and lifetime.[1,2] Metal–air cells have garnered attention as potential high-performance power sources for electronic devices.[3,4] Of these, lithium–air cells are the most promising for high persistence applications.[5,6] However, lithium is too sensitive to ambient conditions such as humidity and oxygen and is a scarce natural resource in some regions.

By contrast, aluminium is an abundant, attractive anode material for energy storage and conversion because of its high specific capacity, highly negative standard electrode potential, and environmentally benign characteristics. Compared with zinc, lithium and other metals, aluminium has its own unique advantages and disadvantages. Its relatively low atomic weight of 26.98 and its trivalence give a gram-equivalent weight of 8.99 and a corresponding electrochemical equivalent of 2.98 Ah g^{-1}, compared with 3.86 Ah g^{-1} for lithium, 2.20 Ah g^{-1} for magnesium and 0.82 Ah g^{-1} for zinc. Moreover, on a volume basis aluminium should yield 8.04 Ah cm^{-3}, compared with 2.06 Ah cm^{-3} for lithium, 5.85 Ah cm^{-3} for zinc and 3.83 Ah cm^{-3} for magnesium.[7]

The barrier to commercialisation is aluminium's high self-corrosion rate in alkaline solutions both under open-circuit conditions and during the discharge process. To reduce the self-corrosion of the aluminium anode, two methods are usually employed: alloying aluminium with other elements[8–10] or modifying the composition of the electrolyte.[11–15] However, little research into industrial Al–air cells has been successful. Thus, we have put

Fuji Pigment Co.Ltd., 2-23-2 Obana, Kawanishi-city, Hyogo Prefecture 666-0015, Japan. E-mail: moriryohei@fuji-pigment.co.jp; Fax: +81-72-7599008; Tel: +81-72-7598501

forward the idea of covering the aluminium anode with a ceramic aluminium ion conductor to prevent anode corrosion due to direct contact with the alkaline electrolyte, while retaining aluminium ion conduction. On the other hand, Zhou *et al.* have placed a solid electrolyte at the air cathode side of a lithium–air cell to prevent oxygen from penetrating the cell, thus inhibiting the formation of Li_2O_2 or Li_2O as the by-product.[16,17] In this study, we have combined both approaches by placing $Al_2(WO_4)_3$ as an aluminium ion conductor, both on the anode and air cathode sides, and succeeded in preparing an Al–air cell with stable cell properties.

Hereafter, we shall refer to this $Al_2(WO_4)_3$ material at anode side as the "film" since its thickness is on the order of 10–20 μm, and the cathode side material as the "lid" due to its thickness of approximately 2 mm and its function as a cover for the liquid electrolyte. For simplicity and comparison, we classify and refer to the Al–air cells presented in this study as follows: (a) aluminium anode + air cathode (AA), (b) aluminium anode + $Al_2(WO_4)_3$ film +
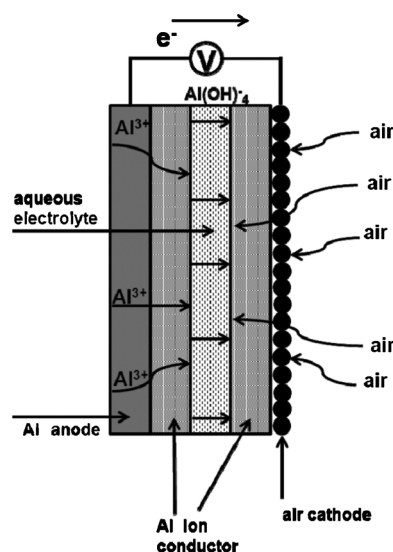
Fig. 1 A schematic figure of AFLA cell.

Fig. 2 Discharge curve of Al–air cells: (a) AA and AFA cells, (b) AFLA cell.

Fig. 3 Charge–discharge curve of the AFLA cell. Discharge curve of the AFLA cell after up to 30 charge–discharge reaction cycles.

air cathode (AFA), and (c) aluminium anode + $Al_2(WO_4)_3$ film + $Al_2(WO_4)_3$ lid + air cathode (AFLA).

A schematic figure of the AFLA cell is given in Fig. 1. The structure of the proposed AFLA cell can be summarized as: "Al|$Al_2(WO_4)_3$|NaOH|$Al_2(WO_4)_3$| air cathode." An aluminium board was used as an anode. The air cathode was composed of acetylene black and polyvinylidenedifluoride (PVDF) dissolved in N-methyl-pyrrolidone on a nickel mesh current collector.

$Al_2(WO_4)_3$ film was prepared by coating the aluminium anode with a printing slurry composed of $Al_2(WO_4)_3$ powder and terpineol, followed by annealing at 600 °C. The $Al_2(WO_4)_3$ lid was prepared by mixing $Al_2(WO_4)_3$ with PVDF and pressing the resulting mixture into a disk. It should be noted here that with this cell structure, we suggest that the major drawback of all metal–air cells, electrolyte evaporation, can be circumvented.

Fig. 2 shows the discharge curve of Al–air cells prepared in this study at an applied current of 0.2 mA cm^{-2}. The capacity of the AA and AFA cells were 17.6 mAh cm^{-2} and 18.9 mAh cm^{-2}, respectively (see Fig. 2 (a)). This relatively small difference allows us to conclude that the $Al_2(WO_4)_3$ film on the Al anode does not significantly influence the cell capacity. Fig. 2 (b) presents the discharge curve of the AFLA cell at an applied current of 0.2 mA cm^{-2}. The capacity of the AFLA cell was 6.9 mAh cm^{-2}, smaller than the AA and AFA cells. Although $Al_2(WO_4)_3$ is an Al^{3+} ion conductor, the thickness of $Al_2(WO_4)_3$ (approximately 2 mm), reduced Al^{3+} ion conduction inside the $Al_2(WO_4)_3$ material, thereby suppressing the cell capacity. However, it is obvious that the AFLA cell functions as a secondary cell.

Fig. 3(a) displays the charge-discharge curve of the AFLA cell at an applied current of 0.2 mA cm^{-2}. The charge-discharge reaction was conducted for approximately one week. To the best of our knowledge, this is the first report on the charge–discharge curves
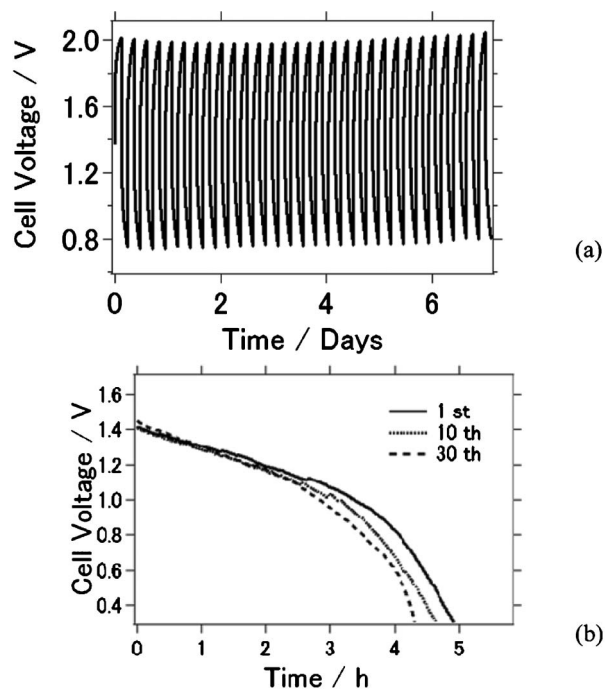
of an Al–air cell for a time period this long.[18,19] However, it should be noted here that because of evaporation of the electrolyte, NaOH solution was refilled once every 2 days to ensure sufficient electrical contact. We suggest that macro and micro pores formed in the lid because of the simple sample preparation technique, and these were responsible for electrolyte evaporation; this will be further discussed in later sections. Fig. 3(b) shows the discharge curve at an applied current of 0.2 mA cm^{-2} for up to 30 charge-discharge cycles at a cut-off potential of 0.3 V. The capacity was initially 5.3 mAh cm^{-2}, but dropped to 5.0 mAh cm^{-2} and 4.4 mAh cm^{-2} at the 10th and 30th cycles, respectively. That is, the capacity did not deteriorate significantly even after 30 charge-discharge reactions.

Nyquist plots of the cells are shown in Fig. 4. The cell resistance difference between AA and AFA cells was small; therefore, the
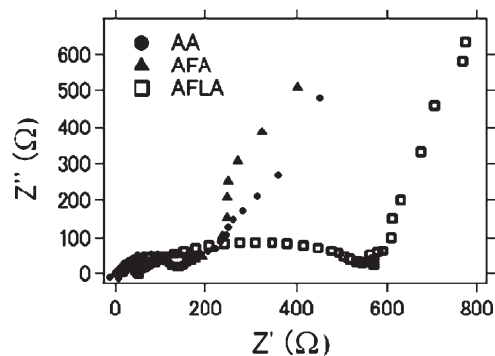
Fig. 4 Nyquist plot of Al–air cells prepared in this study.
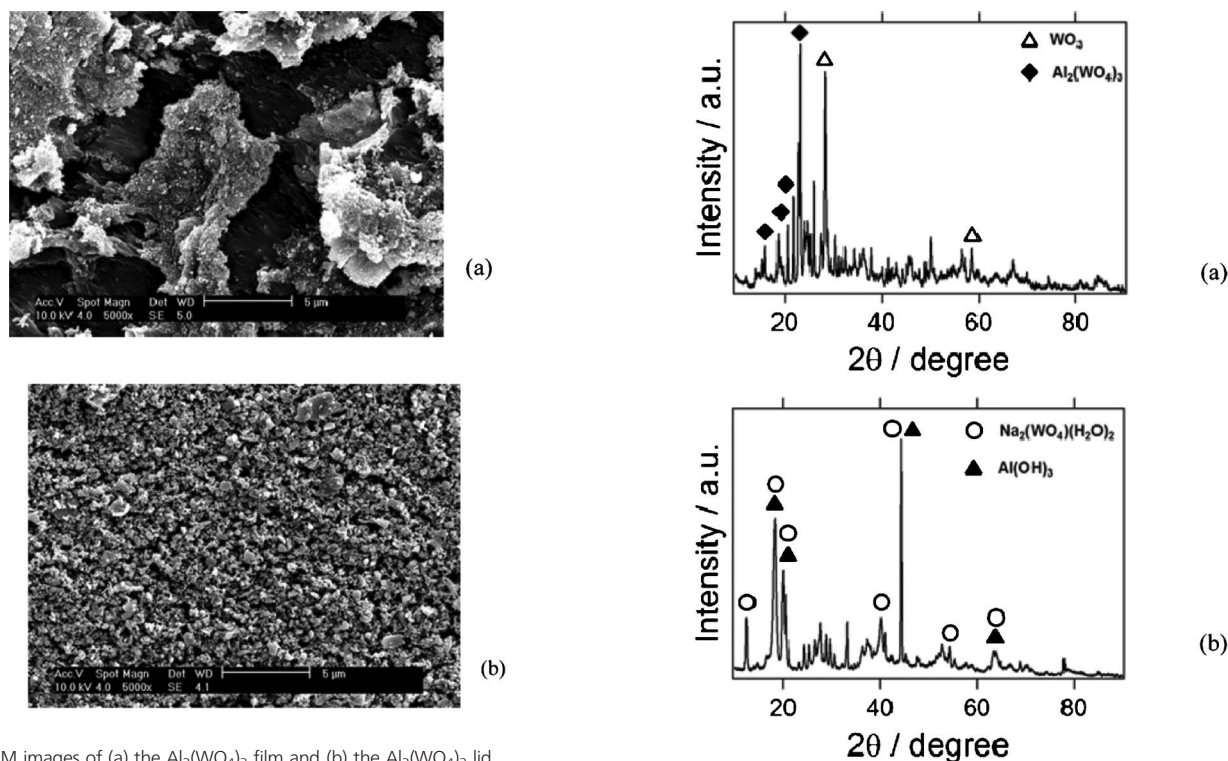
Fig. 5 SEM images of (a) the $Al_2(WO_4)_3$ film and (b) the $Al_2(WO_4)_3$ lid.

resistance of the $Al_2(WO_3)_4$ film is suggested to be small and does not affect the cell resistance. This is probably why the cell capacity difference was also small (see Fig. 2 (a)). However, the cell resistance of AFLA was obviously than the other two cells. This could be attributed to the resistance of the $Al_2(WO_3)_4$ lid, since the thickness of $Al_2(WO_3)_4$ lid is about 2 mm, its resistance was much greater than the $Al_2(WO_3)_4$ film. The intrinsic conductivity of $Al_2(WO_3)_4$ is nearly 4×10^{-6} S cm^{-1} at 600 °C.[20] It should be noted here that the resistance of the $Al_2(WO_3)_4$ lid should be even larger than the measured data in Fig. 4 due to its thickness and intrinsic conductivity. We suggest that this is due to NaOH penetration into the $Al_2(WO_3)_4$ lid, decreasing the overall resistance due to its own liquid electrolyte conductivity. This is also good evidence for electrolyte evaporation *via* macro and micro pores in the lid, as discussed earlier.

Fig. 5 shows SEM images of the $Al_2(WO_4)_3$ film and lid. As seen in Fig. 5(a), the particle sizes range from 100 nm to 2 μm, and the particles are uniformly dispersed on the $Al_2(WO_4)_3$ film surface. It is inferred that owing to this uniform monolith film-like structure, the $Al_2(WO_4)_3$ film resistance was small. On the other hand, the structure and surface of the $Al_2(WO_4)_3$ lid are more rugged and exhibit micro-cracks (Fig. 5(b)). One can conclude the ion conductivity could be improved by preparing a thinner and more densely packed lid, with smaller dispersed particles. In this study, the $Al_2(WO_4)_3$ lid was prepared by simple compression of commercially available $Al_2(WO_4)_3$ powders. By applying appropriate dispersion techniques to break down individual aluminium ion conductor ceramics into small nanoparticles, one can expect to prepare a densely packed $Al_2(WO_4)_3$ lid which would
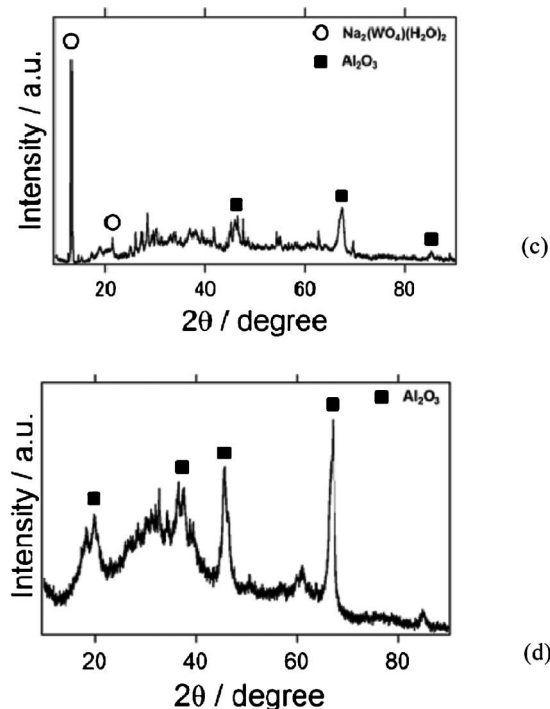
Fig. 6 X-ray diffraction pattern of materials prepared in this study: (a) $Al_2(WO_4)_3$ powder purchased for this study, (b) $Al_2(WO_4)_3$ film after charge–discharge reaction for 3 days with 1.5 M NaOH electrolyte, (c) $Al_2(WO_4)_3$ lid after charge–discharge reaction for 3 days with 1.5 M NaOH electrolyte, (d) $Al_2(WO_4)_3$ lid after soaking in 1.5 M NaOH for 3 days.

demonstrate a higher ion conductivity.[21] This lid preparation method may also prevent electrolyte evaporation.

Fig. 6 displays the X-ray diffraction patterns of the $Al_2(WO_4)_3$ powder, film, and lid after each experiment. Fig. 6(a) shows the X-ray diffraction pattern of the commercially available $Al_2(WO_4)_3$ powder used in this study, which was composed of $Al_2(WO_4)_3$ and WO_3 phases. After 3 days of charge-discharge experiments, the film was composed of $Na_2(WO_4)(H_2O)_2$ and $Al(OH)_3$, as shown in Fig. 6(b). $Al(OH)_3$ formation in the Al–air cell during the charge-discharge reaction can be explained by the following consecutive reactions.

The discharge reaction at the aluminium anode can be written as:

$$Al + 4OH^- \rightarrow Al(OH)^-_4 + 3e$$
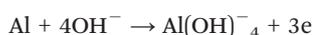
while at the air cathode, the water in the electrolyte reacts with oxygen from the air:

$O_2 + 2H_2O + 4e^- \rightarrow 4OH^-$ Hence, the overall Al–air cell reaction would be:

$$4Al + 3O_2 + 6H_2O + 4OH^- \rightarrow 4Al(OH)_4^-$$
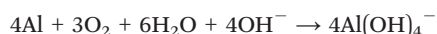
Eventually, aluminium hydroxide precipitates:

$$Al(OH)_4^- \rightarrow Al(OH)_3 + OH^-$$

Fig. 6(c) presents the result for the $Al_2(WO_4)_3$ lid after 3 charge–discharge cycles. $Na_2(WO_4)(H_2O)_2$ and Al_2O_3 were formed instead of the $Al(OH)_3$ phase. It is surprising that $Na_2(WO_4)(H_2O)_2$ was formed after the charge–discharge reaction and $Al_2(WO_4)_3$ was no longer observed. In contrast, simply soaking the $Al_2(WO_4)_3$ lid in 1.5 M NaOH for 3 days, resulted in a pure Al_2O_3 phase, as presented in Fig. 6(d). This means that Al was replaced with Na to form $Na_2(WO_4)(H_2O)_2 \cdot Al_2(WO_4)_3$ which is a known inorganic ion exchanger.[22,23] However, the crystalline phase would not change just by adsorbing metallic ions onto the surface. Generally, the Al^{3+} ion can be easily replaced with other metallic ions *via* conventional solid-state reactions.[24] In the present case, however, a different crystalline phase was formed by electrochemical reaction rather than by a solid-state reaction. Substitutional solid solution by an electrochemical reaction is very rare, especially for inorganic oxide materials, and very few cases have been reported.[25]

Indeed, Adachi *et al.* have reported that $Al_2(WO_4)_3$ can be doped by (Lu) and (Eu) ions by biasing the voltage between $Al_2(WO_4)_3$ and $Ln_2(WO_4)_3$ (Ln = Lu, Eu) in direct contact. They also insisted that with this electrochemical doping procedure, metal doping can be achieved even if the ion radii differ, which is impossible by conventional solid-state reactions (Al^{3+}: 0.0675 nm, Lu^{3+}: 0.1001 nm, Eu^{3+}: 0.1030 nm).[26] The same reaction could be expected in the present study since Na^+ radii is 0.102 nm.[27] Adachi *et al.* claim that they were the first to discover this phenomenon, namely, electrochemical doping of inorganic oxide materials; we utilized this to create a new type of Al–air secondary cell. Since we only observed the Al_2O_3 phase after soaking the $Al_2(WO_4)_3$ lid in NaOH, a completely different process must have occurred *via* the electrochemical reaction. Apart from these suggestions, one could

also infer that the Al ion was dissolved and released into aqueous NaOH, and Na was replaced with Al *via* an electrochemical reaction from the electrolyte. Conversely, the Na^+ ion in NaOH reacted with WO_3 in the commercial powder to form $Na_2(WO_4)(H_2O)_2$. Further research is necessary to understand this phenomenon. One should note that $Al(OH)_3$ and Al_2O_3 were still produced as by-products, which are the major inhibitors for the charge-discharge reaction. However, the present Al–air cell worked for one week, which is longer than any other period reported to date.

In summary, we successfully assembled a functional Al–air cell by placing the aluminium ion conductor $Al_2(WO_4)_3$ both on top of the aluminium anode and underneath the air cathode. We are currently extending the working period of the device to more than a week by applying another electrolyte or aluminium ion conductor with better Al^{3+} ion conductivity.[28,29] Most importantly, one can consider using aluminium as a secondary cell material, as it is more abundant, safer, and easier to handle than other metals such as lithium, zinc, magnesium, and sodium.

Acknowledgements

References

1 R. Padbury and X. Zhang, *J. Power Sources*, 2011, **196**, 4436–4444.

2 J. Chen, J. S. Hummelshøj, K. S. Thygesen, J. S. G. Myrdal, J. K. Nørskov and T. Vegge, *Catal. Today*, 2011, **165**, 2–9.

3 P. Kichambare, J. Kumar, S. Rodrigues and B. Kumar, *J. Power Sources*, 2011, **196**, 3310–3316.

4 M. Armand and J. Tarascon, *Nature*, 2008, **451**, 652–657.

5 G. Girishkumar, B. McCloskey, A. Luntz, S. Swanson and W. Wilcke, *J. Phys. Chem. Lett.*, 2010, **1**, 2193–2203.

6 F. Wagner, B. Lakshmanan and M. Mathias, *J. Phys. Chem. Lett.*, 2010, **1**, 2204–2219.

7 Q. Li and N. Bjerrum, *J. Power Sources*, 2002, **110**, 1–10.

8 S. Abedin and A. Saleh, *J. Appl. Electrochem.*, 2004, **34**, 331–335.

9 M. Krishnan and N. Subramanyan, *Corros. Sci.*, 1977, **17**, 893–900.

10 M. Paramasivam and S. Iyer, *J. Appl. Electrochem.*, 2001, **31**, 115–119.

11 D. Macdonald and C. English, *J. Appl. Electrochem.*, 1990, **20**, 405–417.

12 H. Shao, J. Wang, Z. Zhang, J. Zhang and C. Cao, *Mater. Chem. Phys.*, 2002, **77**, 305–309.

13 Y. Ein-Eli, M. Auinat and D. Starrosvetsky, *J. Power Sources*, 2003, **114**, 330–337.

14 A. Maayta and N. Al-Rawashdeh, *Corros. Sci.*, 2004, **46**, 1129–1140.

15 A. Mukherjee and I. Basumallick, *J. Power Sources*, 1996, **58**, 183–187.

16 E. Yoo and H. Zhou, *ACS Nano*, 2011, **5**, 3020–3026.

17 Y. Wang and H. Zhou, *Environ. Sci.*, 2011, **4**, 1704–1707.

18 A. A. Mohamad, *Corros. Sci.*, 2008, **50**, 3475–3479.

19 M. Nestoridi, D. Pletcher, R. J. K. Wood, S. Wang, R. L. Jones, K. R. Stokes and I. Wilcock, *J. Power Sources*, 2008, **178**, 445–455.

20 Y. Kobayashi, T. Egawa, S. Tamura, N. Imanaka and G. Adachi, *Chem. Mater.*, 1997, **9**, 1649–1654.

21 R. Mori, T. Ueta, K. Sakai, Y. Niida, Y. Koshiba, L. Lei, K. Yamaguchi, K. Nakamae and Y. Ueda, *J. Mater. Sci.*, 2011, **46**, 1341–1350.

22 Z. A. Othman, M. Naushad, M. Khan and S. Wabaidur, *J. Inorg. Organomet. Polym. Mater.*, 2012, **22**, 352.

23 M. Naushad, *Bull. Mater. Sci.*, 2008, **31**, 957–965.

24 J. Köhler, Y. Kobayashi, N. Imanaka and G. Adachi, *Solid State Ionics*, 1998, **113–115**, 553–558.

25 V. Ozeryanskaya, V. Gaterman, I. Shukaey and V. Grigorev, *Russ. Chem. Bull.*, 1998, **47**, 1481–1486.

26 N. Imanaka, M. Hiraiwa, S. Tamura and G. Adachi, *Electrochem. Solid-State Lett.*, 1999, **2**, 570–571.

27 Y. Jia, *J. Solid State Chem.*, 1991, **95**, 184–187.

28 N. Imanaka and S. Tamura, *Bull. Chem. Soc. Jpn.*, 2011, **84**, 353–362.

29 N. Imanaka, Y. Hasegawa, M. Yamaguchi, M. Itaya, S. Tamura and G. Adachi, *Chem. Mater.*, 2002, **14**, 4481–4483.